This manuscript was accepted by Rev. Sci.Instrum. Click here to see the version of record.

Dual-pass upgrade to the Thomson Scattering diagnostic on the Prototype Material Plasma Exposure eXperiment[a)]

N. Kafle,[1,2,b)] T.M. Biewer,[2] and D.C. Donovan[1]
[1)]*Nuclear Engineering, The University of Tennessee, Knoxville, TN 37996*
[2)]*Oak Ridge National Laboratory, Oak Ridge, TN 37831*

(Dated: 6 June 2018)

The Thomson scattering (TS) diagnostic on the Proto-MPEX has been upgraded to measure electron temperature (T_e) and density (n_e) simultaneously at two axial locations. After the first pass through the vacuum vessel, the exiting laser beamline is re-collimated in atmosphere and rerouted into the vacuum vessel for the second pass. The upgrade will help diagnose axial T_e and n_e gradients between the 'central chamber' and the target region, which are located 1 m and 2.5 m, respectively, downstream from the Helicon radio-frequency (RF) source. TS measurements have given $T_e \approx 4-15$ eV and $n_e \approx 2-4\times10^{19}$ m^{-3} at the central chamber, and $T_e \approx 1-2$ eV and $n_e \approx 1-2\times10^{19}$ m^{-3} at the target. The upgrade also increases the number of sampling points at the target from 3 fibers to 5 fibers, measuring 3 cm radially across the plasma column, and 25 fibers in the central chamber radially spanning 8 cm. The intensified CCD camera is double triggered for each laser pulse: 1) to measure the TS and laser stray light, and 2) to measure the plasma background light, which contains nuisance emission lines and bremsstrahlung. Subtracting the background light from the TS photons improves the temperature and density measurements. Details of the diagnostic setup, axial and radial measurements, and areas for further optimization are discussed.

Keywords: Linear device, dual-pass Thomson Scattering, electron temperature, electron density

I. INTRODUCTION

The Material Plasma Exposure Experiment (MPEX)[1,2], once completed, will be one of the preeminent user facilities to study plasma materials interaction in tokamak 'divertor-like' conditions. Helicon radio-frequency (RF) plasma source development along with auxiliary heating, such as electron cyclotron heating (ECH)/electron Bernstein wave (EBW) and ion cyclotron heating (ICH) is currently being demonstrated in Proto-MPEX at Oak Ridge National Laboratory. Thomson scattering[3–7] (TS), which is non-perturbative, is one the primary diagnostics that uses an active spectroscopic technique to measure the fundamental plasma parameters such electron temperature and density with high spatial resolution. A detail discussion of the Thomson scattering laser system, initial implementation and first results in Proto-MPEX can be found elsewhere[8,9].

The existing Thomson scattering laser beam is recycled from the target region to the 'central chamber,' for the second pass. The motivation for the dual-pass laser system arose to replace perturbative diagnostics such as Langmuir probes with a robust and non-invasive diagnostic system at multiple axial locations. Langmuir probes can suffer physical damage in the presence of high localized heat fluxes from auxiliary heating, and since they also depend on simplifying assumptions in a magnetic field, they can be difficult to interpret when attempting to measure electron temperatures and densities from ECH/EBW and ICH. The availability of only one Nd:YAG laser entailed the need to recycle the laser beam. This paper will present a brief description of the Thomson scattering diagnostic hardware in Proto-MPEX in Sec. II, a detail description of the second laser beamline installation in Sec. III, the results of the measurement from two locations in deuterium plasma discharges in Sec. IV, and conclude with a summary and discussion of further improvement in Sec. V.

II. THOMSON SCATTERING DIAGNOSTICS HARDWARE

Proto-MPEX uses a Newport Quanta-Ray Pro 350-10 Hz laser system for its Thomson scattering diagnostics to measure electron temperature and density pulsed every 100 ms during a plasma shot. The fundamental wavelength of the Nd:YAG laser system is at 1064 nm, and when the laser is passed through the potassium di-hydrogen phosphate (KD*P) crystals it is frequency doubled to produce light at half the wavelength (532 nm). The maximum energy output from the laser is up to 1.4 J per 8 ns pulse. A PI MAX III intensified charge coupled device (ICCD) camera with generation III intensifier from Princeton Instruments is used to collect the scattered signal through a Kaiser Optical Systems Holospec f/1.8 spectrometer. Ideally, the fiber coupled intensifier is gated to $\geq$ 10 ns to reduce bremsstrahlung emission detection. However, functionally a gate width of 70 ns or higher is required to accommodate timing jitter of the triggering system, and to allow light to travel back from the machine to the spectrometer. Since the light is transported by two fiber bundles of differing lengths, the minimum gate width is effectively 100 ns to reliably record photon counts.

III. SECOND-PASS LASER IMPLEMENTATION

Multiple axial measurement[5] of plasma parameters using Thomson scattering has been implemented in other linear devices, but the upgrade in Proto-MPEX enables simultaneous

[a)]Paper published as part of the Proceedings of the 22nd Topical Conference on High-Temperature Plasma Diagnostics, San Diego, California, April, 2018.
[b)]Author to whom correspondence should be addressed: nkafle@vols.utk.edu

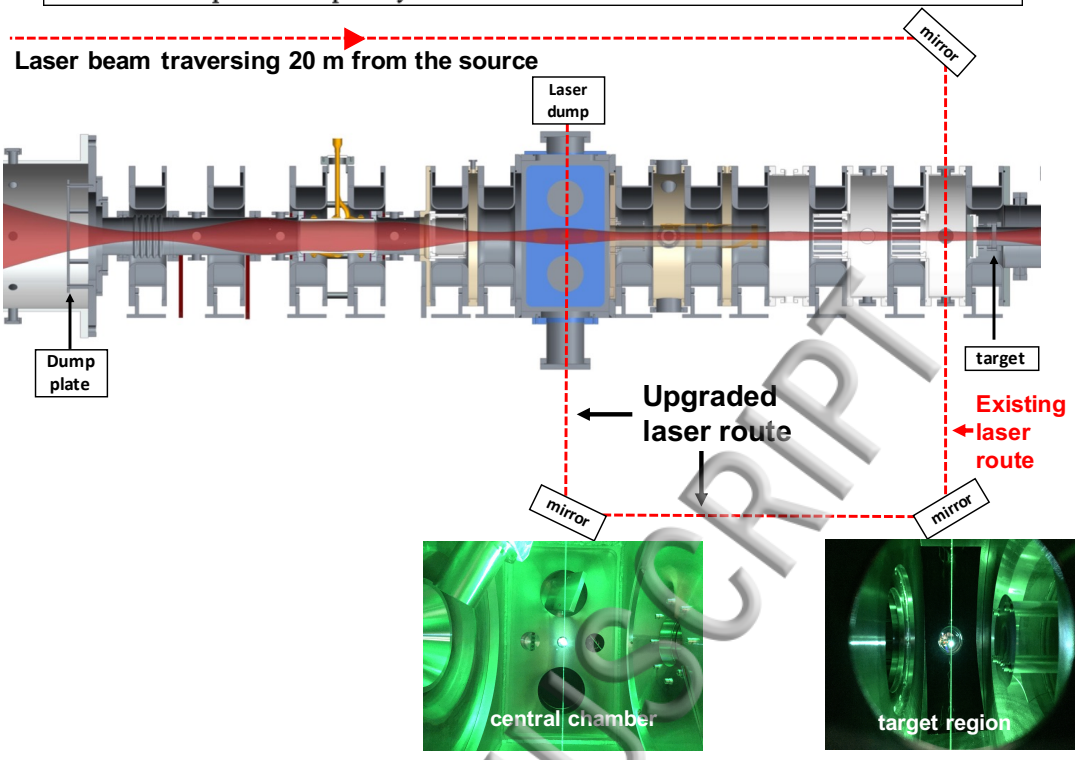

FIG. 1. Laser route through the Proto-MPEX vacuum chamber is depicted. The laser route near the target chamber existed previously and the additional laser route from the 'central chamber' has been added recently. The axial variation in the plasma diameter due to changing magnetic field is depicted by the red surface. The photographs at the bottom show the air breakdown occurring at the focal point at the geometric center of the (vented) vacuum chamber.

measurement of axial electron temperature and density gradients between the central chamber and the target region, which will allow us to observe gradients in plasma parameters necessary for plasma transport studies.

Figure 1 depicts a picture of the laser route (red dotted line) passing through two axial locations in the Proto-MPEX vacuum chamber. Fig. 2 shows the detailed optical arrangement of the Thomson scattering diagnostics system, and the Nd:YAG laser path from the laser source to the dump in Proto-MPEX. The laser traverses ∼20 m from the source, located at the diagnostics laboratory, to the target region for the first pass through the vacuum vessel. The beam diameter set by amplifier rod at the source output is about ∼13 mm, which is doubled using a Galilean beam expanding telescope (BET), as depicted in Fig. 2. The figure also shows the position of six, 50.8 mm diameter, high energy Nd:YAG/Nd:YLF laser steering mirrors (represented as M_1-M_6) from CVI Laser Optics. All but one mirror (M_6) has remote steering capability. Remote actuators from Thor Labs (PIAK10) with 10 mm of travel range are used to control two axes motion. A 50.8 mm diameter laser grade Plano-convex spherical lens (focal distance, f_d = 1500 mm) from CVI Laser Optics is used to focus the beam at the midplane of the vacuum chamber. Without the focusing lens the beam diameter would be ∼30 mm at M_3 before entering the vacuum vessel. As mentioned elsewhere[9], the focusing lens serves two purposes: 1) it enables the laser beam to pass through the standard 70 mm conflat-flanged vacuum tube, which has an inner diameter of 35 mm, and 2) it focuses the laser beam to a small scattering volume to get a localized measurement. There are four apertures installed in the flight tubes for the first pass to reduce the stray light from the "Brewster angled" window, labeled as A_1-A_4 to reduce the stray light count. Apertures A_1, A_4 have 25 mm diameter, and A_2, A_3 have 20 mm diameter.

For the dual-pass upgrade, the existing laser beam, after exiting from the vacuum vessel in the target region, has been directed towards the 'central chamber' using two turning mirrors (M_4 and M_5). The laser dump was removed from under the vacuum vessel at the target region, and replaced by a turning mirror (M_4). The mirror steers the laser beam parallel to the vessel towards the central chamber. At the exit of the laser enclosure box, the diverging laser beam is re-collimated using a laser grade Plano-convex spherical lens, and refocused, 1 m downstream, using another Plano-convex lens (f_d = 1500 mm). The laser beam is then steered into the vacuum chamber with another remote steerable turning mirror (M_5). The horizontal distance between the target region and the central chamber is measured to be about 1.5 m. Two Brewster angled windows, similar to that used for the first-pass has been installed for the second pass to minimize the reflection. All four vacuum to air Brewster window (BW_1-BW_4) interfaces used in Proto-MPEX are depicted in Fig. 2. However, due to the limited available space, the vibration mitigation bellows and electrical isolation ceramic breaks, which would electrically and mechanically isolate the beam enclosures from Proto-MPEX, could not be installed for the second pass. Furthermore, the vacuum chamber at the central chamber shapes as a large rectangular box for the auxiliary heating components, and in addition, a 203 mm diameter, 280 mm long conflat cross attached at the bottom leaves negligible space for aperture to be added for the second pass. After exiting Proto-MPEX for the second time, the laser is dumped

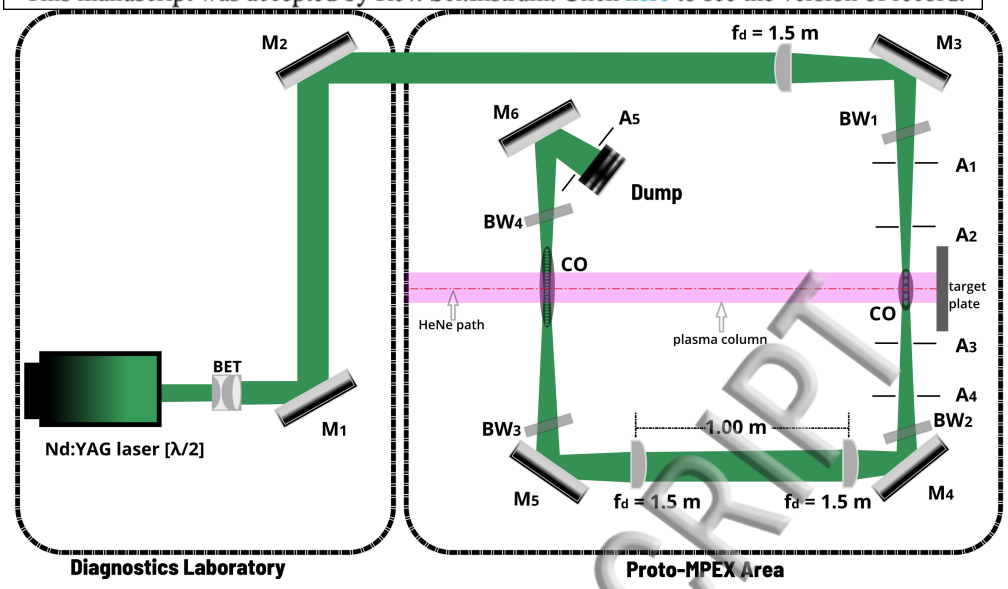

FIG. 2. Thomson scattering diagnostics optical arrangement and the laser path from the diagnostics laboratory to Proto-MPEX (not to scale). In the figure, **BET**: beam expanding telescope, $\mathbf{M_1}$-$\mathbf{M_6}$: mirrors, **CO**: collection optics, $\mathbf{A_1}$-$\mathbf{A_5}$: aperture, and **BW**: Brewster window.

over a stack of stainless steel razor blades in the laser dump.

Two different sets of collection fiber optics (CO) are installed in Proto-MPEX to collect scattered photons: a 5×3 bundle in the target region and a 25×1 bundle at the central chamber. At the focal point the laser diameter is <1 mm which only permits the use of one column of the fiber optics in the target region, but the other two columns are used for passive spectroscopic diagnostics. Moreover, the upgrade has also increased the sampling point from 3 fibers to 5 fibers measuring 3 cm radially across the plasma column in the target region. The newly installed 25 optical fiber bundle at the central chamber spans 8 cm across the plasma radius. The collection diameter of each fiber optic is 400 microns for the near target bundle and 200 microns for the central chamber bundle and the numerical aperture (NA) is 0.37, and the solid angle obtained by the collection optics at the first pass is ~ 0.47 sr, and the second pass is ~ 0.14 sr. The optical fiber bundles can be translated vertically to measure different radii as required by the nature of the experiment. Due to the limitation of the spectrometer, only a total of 20 sampling points can be used at a given time (typically 15 at the central chamber and 5 at the target region). The transfer to the spectrometer is done using an optical patch panel with SubMiniature version A (SMA) connectors.

To identify the vertical position of the collection optics and the horizontal position of the laser beam with respect to the center of the plasma column, an ad hoc method was implemented. A Class I helium-neon (HeNe) laser was projected from the center dump plate to the center of the target, which defined the axis of the plasma column, as shown by the dotted (red) line in Fig. 2. The HeNe was project on the target plate where the plasma hot spot was observed. The point where the Nd:YAG, HeNe and the focused collection optics met gave the alignment of the laser beam and the collection optics with respect to the axis of the plasma column.

Prior to the upgrade, the laser source, which is about $\sim$ 20 m, was presumed to at an infinite distance away, so the focusing lens was initially placed approximately 1.5 m upstream from the chamber axis at the target region. However, the high power densities on the lower "Brewster angled" window (BW_2) was regularly impairing the window. Using the lens equation (Eq. 1),

$$\frac{1}{f_d} = \frac{1}{o_d} + \frac{1}{i_d}, \tag{1}$$

where o_d and i_d are object and image distances, respectively, and accounting for the source distance of $\sim$ 20 m, the beam focus was calculated to be at 1.62 cm, which was 12 cm below the midplane. The lens was moved to 1.62 m upstream from the chamber axis for the first pass to maintain the laser focus at the chamber midplane. Similarly, for the second pass focusing was occurring 14 cm above the midplane; therefore the lens was place 1.64 m upstream from the machine axis. After rectifying the lens position, the air breakdown occurring at the machine axis at both locations was observed when vented to atmosphere, as shown in Fig. 1. Additional complications have surfaced with the upgrade of the second pass. The movement of the laser beam on the second pass through the vacuum vessel has been observed when the magnetic field is applied on Proto-MPEX; causing it to misalign with the collection fiber optics bundle. Any small movement in the laser beam anywhere upstream could severely be exaggerated when making the second pass; therefore making the probability of maintaining the laser alignment for the second pass even smaller. The process to identify the cause of the movement is still in progress, but presently the Rayleigh scattering calibration with nitrogen is conducted in the presence of the magnetic field to account for any movement the may be present during plasma discharges.

The noise on the signal arriving at the collection optics from the laser stray light and the plasma background is always a challenge with a Thomson Scattering diagnostics. In order to reduce the optical noise a significant portion of the vacuum chamber and the laser flight tubes has been covered with Acktar Spectral Black foil at both locations. Similarly, reflecting surfaces at the central chamber, which are used for

microwave injection are anodized with black coating. The laser dump is placed at ∼40° — 50° angle to minimize the light reflecting back into the flight tube. An iris with an adjustable aperture (A_5), as shown in Fig. 2, is placed in front of the laser dump to minimize the scattered light back into the laser flight tube. Moreover, subtraction of the nuisance emissions and bremsstrahlung is done by triggering the ICCD camera twice, during and 20 ms after the laser pulse, using Stanford Research Systems pulse generator. With this technique, plasma background light and the stray light can be measured separately from the Thomson scattering signal. Typically, an ensemble of 5-10 discharges is required to obtain a reliable electron temperature and density profile. Moreover, to improve the statistics, and to remove the noise 2× or 4× pixel binning in the wavelength axis of the ICCD camera has been implemented. The pixel binning in the wavelength axis reduces the signal-to-noise ratio and increases the ICCD readout frequency[7].

IV. RESULTS FROM DUAL-PASS DEUTERIUM PLASMA

The increase in signal-to-noise ratio and advancement in the machine performance has vastly improved the Thomson scattering diagnostics in Proto-MPEX. The number of shots required for an ensemble has been reduced from ∼ 40 shots to ∼ 10 in high electron density ($2-5\times10^{19}$ m^{-3}) deuterium discharges. The spectrometer background is about 1300 counts. However, using the double triggering technique, the plasma background count for the 100 ns gated width was observed to have a minuscule contribution to the optical noise when compared to the instrumentation noise and the laser stray light. Moreover, from the Rayleigh scattering calibration the stray light limited lowest measurable density was calculated to be 1.5×10^{18} m^{-3}. Fig. 3 shows a fit to Thomson scattering data obtained from a fiber at r = -1.5 cm from the target region. In Fig. 3a), the fitted Thomson photon counts are represented by the blue dots, and the Gaussian fit is presented by the red line. The stray light count still dominates the collected Thomson scattering photons; therefore, the center of the laser light near the laser wavelength (532 nm) is masked during the Gaussian fitting process. Excluded data around 532 nm are shown by open circles in the figure. Fig. 3b) shows the residual to the fit, where the open circles are again the excluded data.

Proto-MPEX has successfully produced high densities plasma with light ions. Results shown here are experiments conducted with deuterium discharges when the magnetic fields were set to ∼ 0.7 T on the main coil, and to ∼ 0.03 T around the Helicon plasma source. Seventeen sampling point at the central chamber, and three sampling points the target region have been used for the presented results. On-axis electron density of $2.05\pm0.26\times10^{19}$ m^{-3} at the central chamber, and $1.23\pm0.17\times10^{19}$ m^{-3} at the target region, with the corresponding electron temperature of 3.96 ± 1.31 eV at the central chamber, and 1.16 ± 0.17 eV at the target region have been measured from the Thomson scattering system. The radial electron temperature and density profiles obtained simultaneously at the target region and the central chamber are shown in Fig. 4 and Fig. 5, respectively. It should be noted that the radius (R) shown in the radial profiles is local

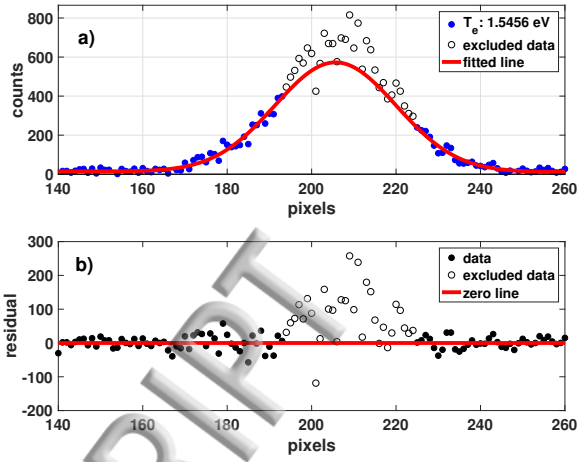

FIG. 3. A fit to the Thomson scattering data from a fiber at the target region is shown. In a) blue dots are the scattered photon counts, open circles are the excluded data around the 532 nm, and the red line is the Gaussian fit to the data. In b) black dots are the residual from fitted data, open circles are the excluded data, and the red line is the zero reference line.

to the measurement locations. Since there is spatial variation in the plasma diameter due to axially changing magnetic field strength[10] in Proto-MPEX (as shown in Fig. 1), a flux tube mapping will necessary to directly compare the electron temperature and density values between the central chamber and the target region.

Using the 95% confidence interval from each coefficient in the Gaussian fit, error is propagated to obtain relative error of the measured electron temperature and density. We estimate that our systematic uncertainty is ∼ 10%. These uncertainties are propagated with the photons and fitting errors as shown here. Near the edge of the plasma the TS scattered counts are negligible, which constitutes for the large error bars in the radial profile obtained at the central chamber. This is depicted in Fig. 2 as some of the optical fibers at the central chamber lie above the plasma column.

V. SUMMARY

The work presented in this paper discusses the major upgrade of the Thomson scattering diagnostics from a single pass system near the target region to a dual-pass system, which adds a new measurement location at the central chamber in Proto-MPEX. The Thomson scattering upgrade gives confidence in the measurement of the plasma parameters at multiple locations in Proto-MPEX. In addition, improvement on the signal-to-noise ratio has increased the efficiency of the diagnostic system. The simultaneous measurement of electron temperature and density can now be used for reliable measurement of the axial plasma gradients in Proto-MPEX. For experiments when the target plate is moved closer to the laser beam, the stray light peak saturates the detector as it exceeds its dynamic range; thus, making it difficult to quantify near target parameters. Also, the added travel length from the upgrade has contributed to the misalignment at the second pass. The small motion and the vibration of one of the mirrors dur-

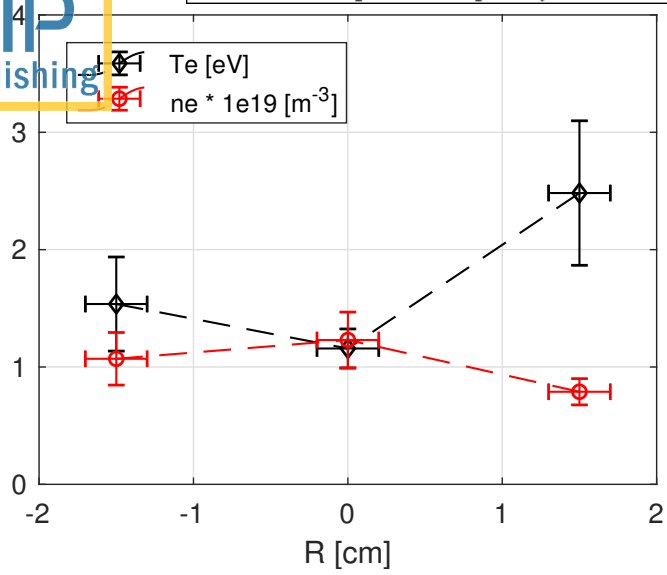

FIG. 4. Electron temperature and density measurement from Thomson scattering near the target region

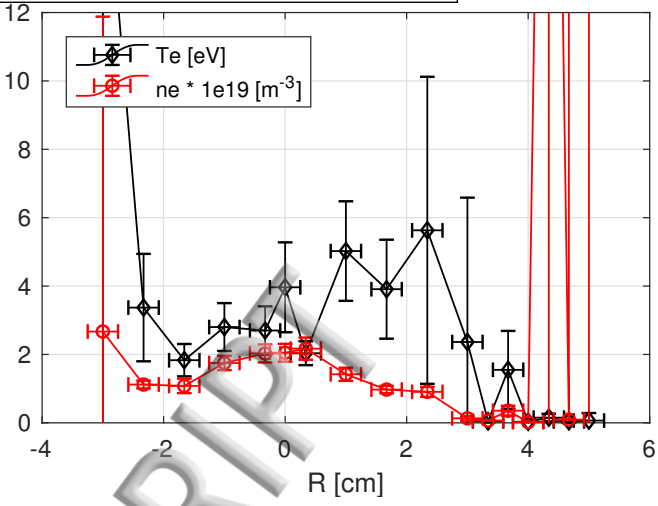

FIG. 5. Electron temperature and density measurement from Thomson scattering at the central chamber

ing plasma discharges could be causing the laser beam to drift away from the intended position, which may have been contributing to the misalignment of the laser with respect to the collection optics. Decoupling the optical components from the magnetic components attached to Proto-MPEX in addition to an active laser beam stabilization should improve the system performance.

ACKNOWLEDGMENTS

This work was supported by the U.S. D.O.E Contract No. DE-AC05-00OR22725. Research sponsored by the Laboratory Directed Research and Development Program of Oak Ridge National Laboratory, managed by UT-Battelle, LLC, for the U.S. Department of Energy.

The authors greatly appreciate the support provided by the Proto-MPEX team, especially: Juan Caneses, John Caughman, Andy Fadnek, Rick Goulding, Jason McDaniel, Juergen Rapp, and Mark Watson, who made this work possible.

[1] J. Rapp, Fusion Science and Technology **72**, 211 (2017).
[2] J. Rapp, T. Biewer, T. Bigelow, J. Caneses, J. Caughman, S. Diem, R. Goulding, R. Isler, A. Lumsdaine, C. Beers, *et al.*, Nuclear Fusion **57** (2017).
[3] D. Evans and J. Katzenstein, Reports on Progress in Physics **32**, 207 (1969).
[4] A. Okamoto, S. Kado, S. Kajita, and S. Tanaka, "Laser Thomson scattering system applicable to low-temperature plasma in the divertor simulator MAP-II," (2005).
[5] H. J. Van Der Meiden, A. R. Lof, M. A. Van Den Berg, S. Brons, A. J. Donné, H. J. Van Eck, P. M. Koelman, W. R. Koppers, O. G. Kruijt, N. N. Naumenko, T. Oyevaar, P. R. Prins, J. Rapp, J. Scholten, D. C. Schram, P. H. Smeets, G. Van Der Star, S. N. Tugarinov, and P. A. Van Emmichoven, Review of Scientific Instruments **83**, 123505 (2012).
[6] M. Hubeny, B. Schweer, D. Luggenhölscher, U. Czarnetzki, and B. Unterberg, Nuclear Materials and Energy **12**, 1253 (2017).
[7] K. Lee, K. Lee, J. Kim, and T. Lho, Review of Scientific Instruments **89**, 013508 (2018).
[8] T. M. Biewer and G. Shaw, Review of Scientific Instruments **85**, 11D812 (2014).
[9] T. M. Biewer, S. Meitner, J. Rapp, H. Ray, and G. Shaw, Review of Scientific Instruments **87**, 11E518 (2016).
[10] N. Kafle, L. Owen, J. Caneses, T. Biewer, J. Caughman, D. Donovan, R. Goulding, and J. Rapp, Physics of Plasmas **25**, 052508 (2018).

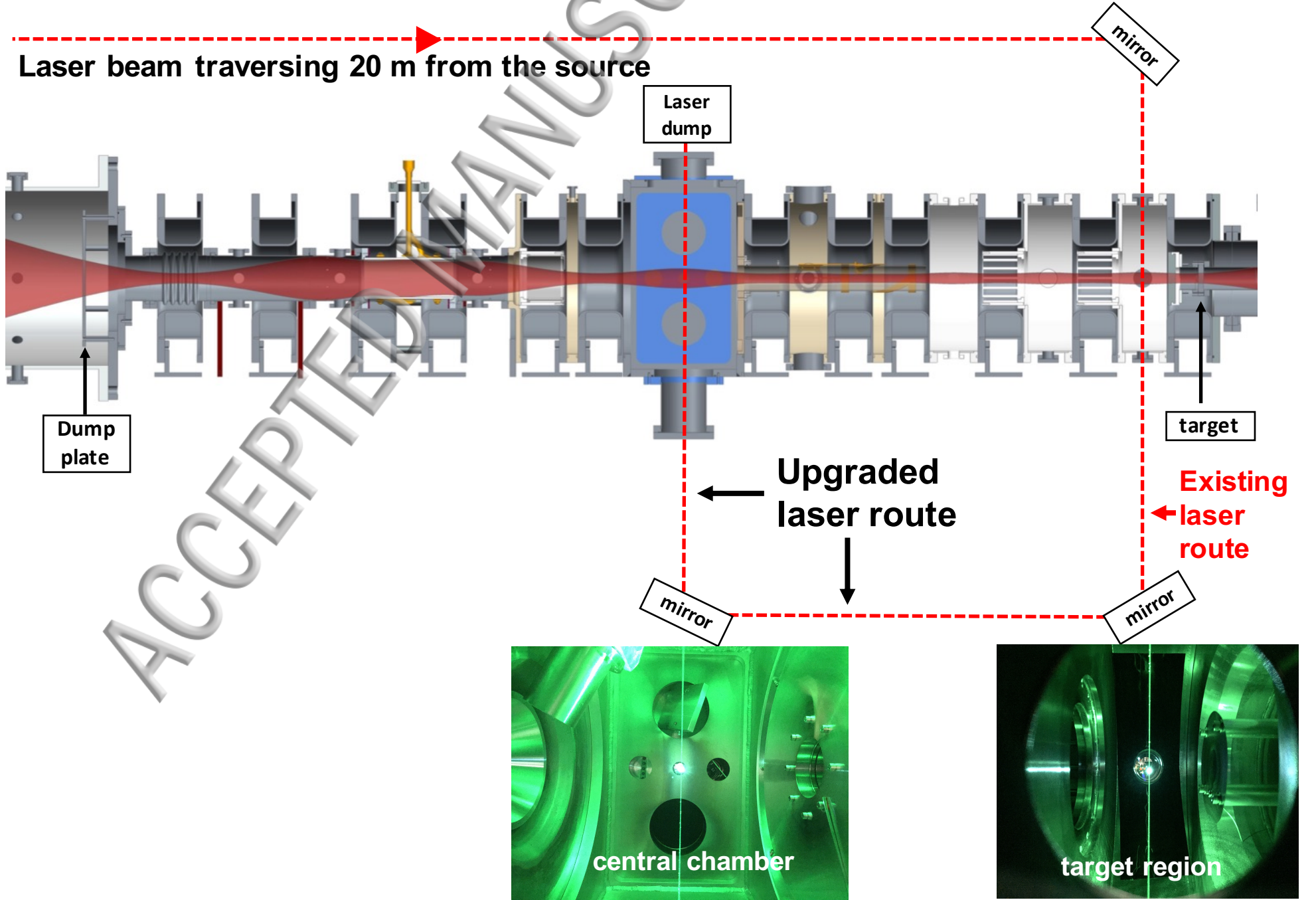

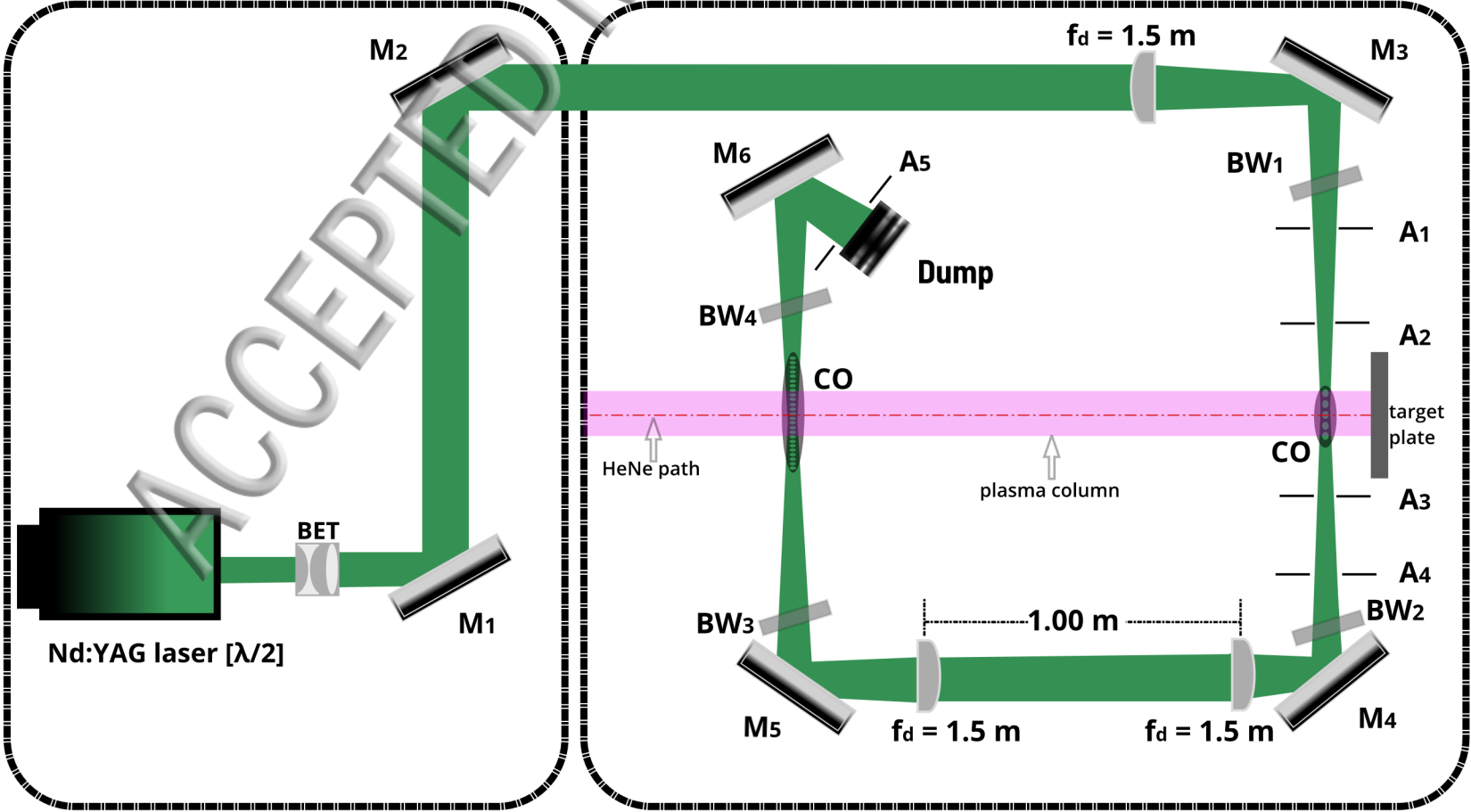
M2
fd = 1.5 m
M3
M6
A5
BW1
A1
Dump
BW4
A2
CO
target plate
HeNe path
plasma column
CO
A3
A4
BW3
1.00 m
BW2
M5
fd = 1.5 m
fd = 1.5 m
M4
BET
M1
Nd:YAG laser [λ/2]
Diagnostics Laboratory
Proto-MPEX Area

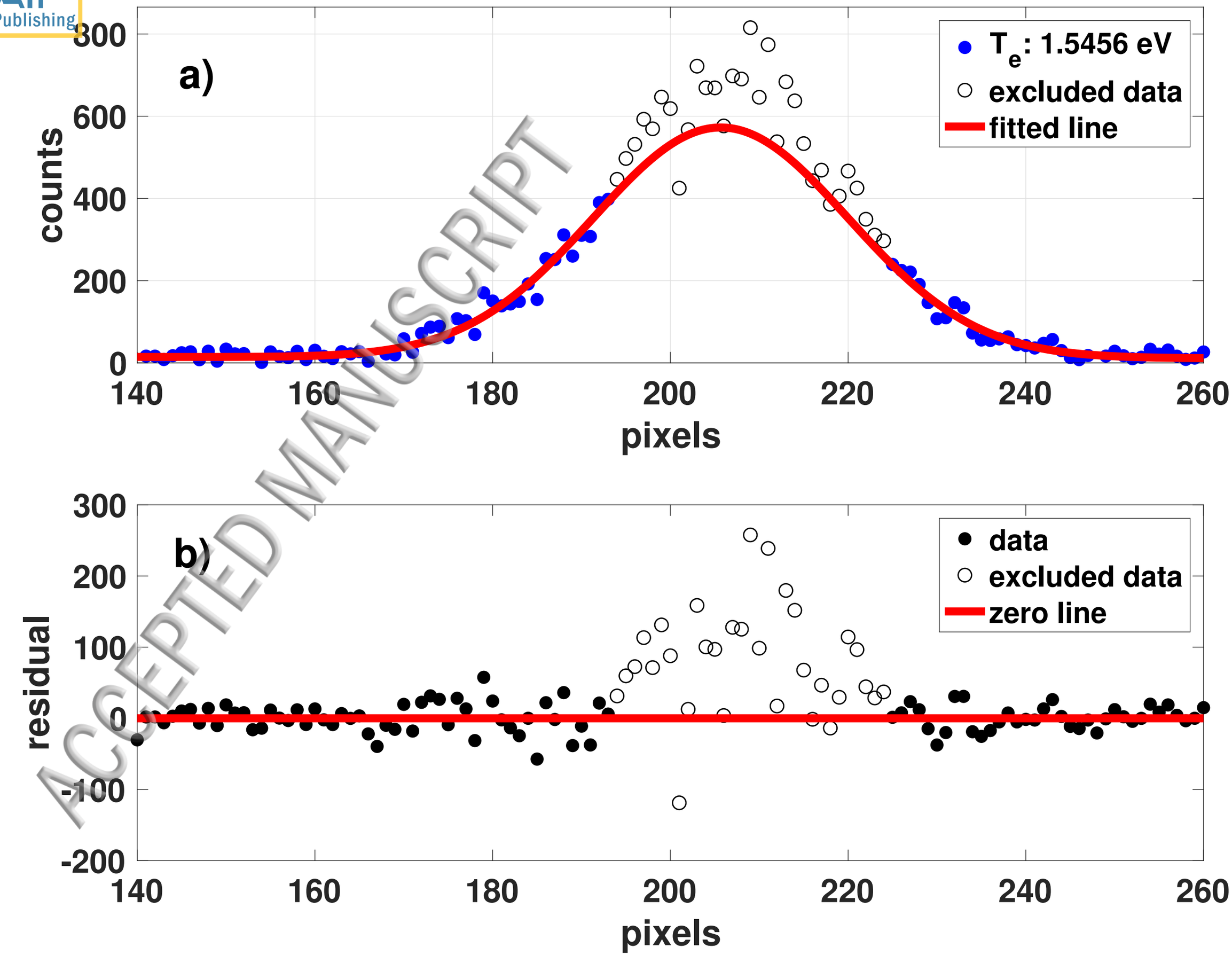

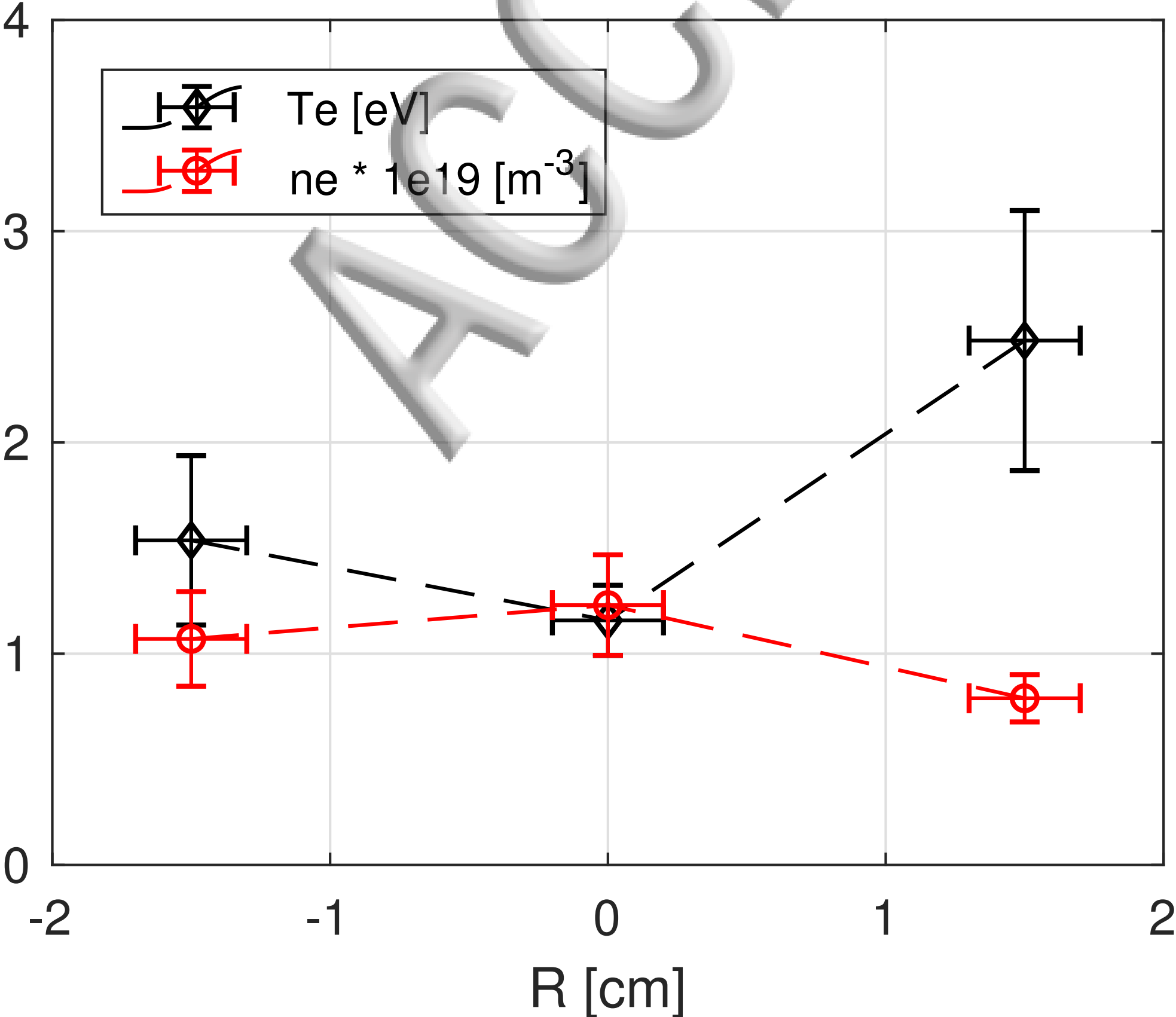
Te [eV]
ne * 1e19 [m-3]
4
3
2
1
0
-2
-1
0
1
2
R [cm]

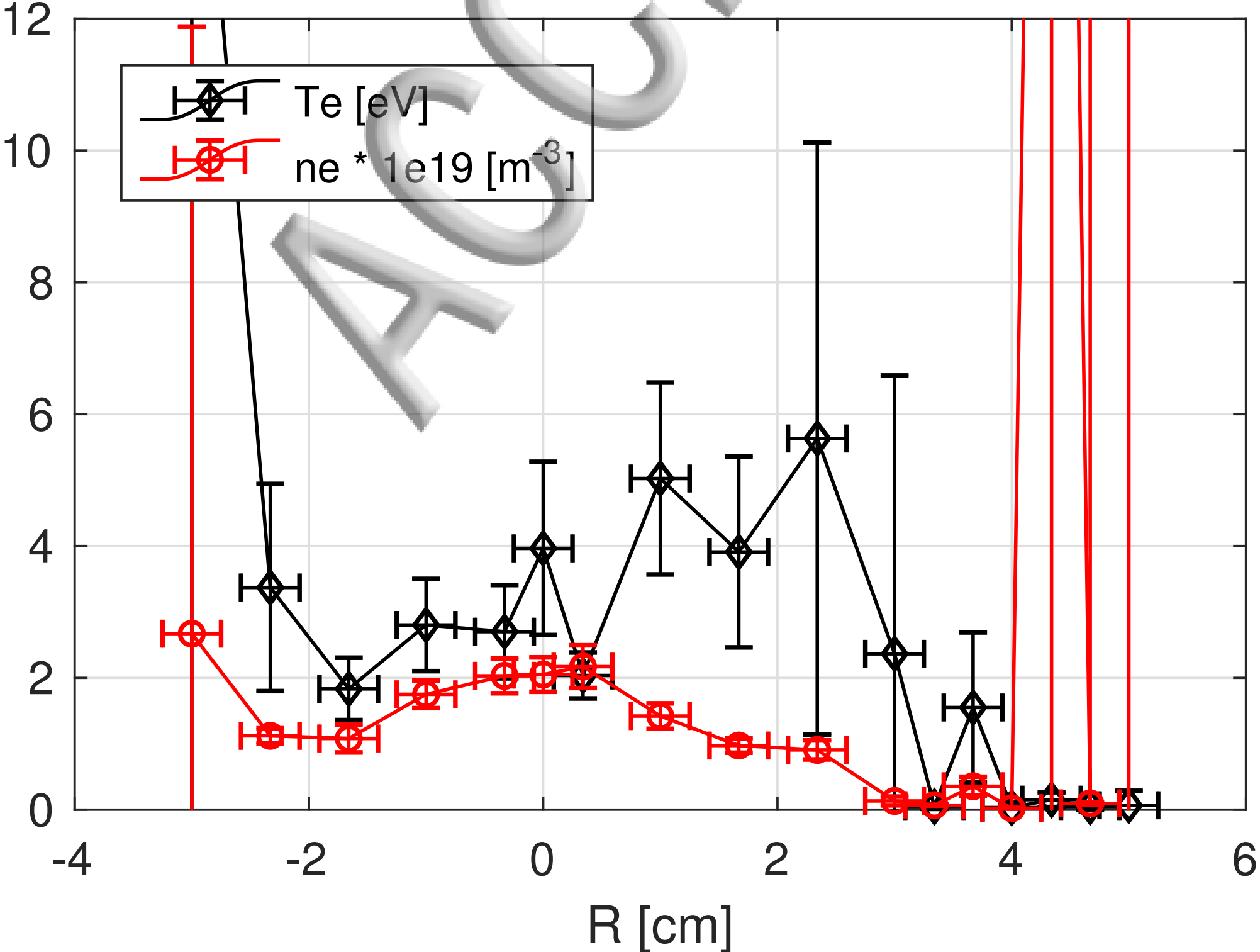
Te [eV]
ne * 1e19 [m-3]
12
10
8
6
4
2
0
-4
-2
0
2
4
6
R [cm]